

INFLUENCE OF ANNEALING TEMPERATURE OF TiO₂ NANOTUBES VIA HYDROTHERMAL METHOD ON Ti FOIL FOR PHOTOCATALYTIC DEGRADATION

Y. SUN^{a,*}, E. D. LIU^b, L. ZHU^c, Y. WEN^a, Q. W. TAN^a, W. FENG^{a,*}

^a*School of Mechanical Engineering, Chengdu University, Chengdu 610106, Sichuan, China*

^b*College of Materials and chemistry & Chemical Engineering, Chengdu University of Technology, Chengdu 610059, Sichuan, China*

^c*School of Chemical Engineering, Yunnan Open University, Kunming 650223, Yunnan, China*

Using Ti foil as titanium source, TiO₂ nanotubes were prepared via a one-step hydrothermal method with heat temperature of 140°C for 6 h in 10 M NaOH solution. The samples calcined at different temperatures were characterized by XRD, SEM, EDX and TEM. As TiO₂ nanotubes calcined at 650°C, anatase phase started to transform to rutile phase. Meanwhile the structure of TiO₂ nanotubes began to be destroyed and the length was shortened. At a calcination temperature of 750°C, the tubular structure is completely disappeared, instead of rod-shaped nanoparticles. Due to the anatase phase composition and the preservation of nanotubes structure, TiO₂ calcined at 450°C exhibited the best photocatalytic activity evaluated by degradation of MB solution.

(Received December 31, 2018; Accepted June 5, 2019)

Keywords: TiO₂ nanotubes, Hydrothermal, Calcination temperature, Photocatalytic degradation

1. Introduction

Due to the unique properties, TiO₂ photocatalyst is widely used in many areas such as hydrogen production [1, 2], water purification [3-5], lithium-ion batteries [6, 7] and dye-sensitized solar cell [8, 9]. As a promising photocatalytic material, TiO₂ has two forms, powder and film. However, the agglomeration and recycle of TiO₂ nanoparticles greatly limit the extensive application of TiO₂ photocatalyst [10]. Hence the immobilization of TiO₂ avoiding above problems could be regarded as a prospective route to photocatalytic application. Comparing with other preparation methods of TiO₂ film [11-14], hydrothermal method demonstrates more advantages and attracts most researchers' attentions. On the one hand, Ti foil, as a titanium source and substrate, could improve the electric conductivity and adhesion of TiO₂ films, which is useful for the photoelectrochemical properties. On the other hand, TiO₂ films with various structures of nanoflowers, nanotubes, nanobelts, nanowires and nanorods, can be achieved with large specific surface [15-19].

As we know, crystal structure, grain size and morphology play an important role in the properties of nano-TiO₂ [20]. At present, most researches focus on the growth regulation of TiO₂ films, including the reaction time [21, 22], reaction temperature [23, 24], the type and concentration of solution [25, 26] during hydrothermal process. There are few reports on the influence of calcination temperature of TiO₂ films fabricated by hydrothermal method. Based on previous researches, TiO₂ nanotubes were synthesis on Ti foil by hydrothermal reaction. The effect of

*Corresponding author: fengwei@cdu.edu.cn

calcination temperature on the crystal structure, morphology and photocatalytic activity of TiO₂nanotubes is investigated in this work.

2. Materials and methods

Pure Ti foil was polished with a mixed solution of HNO₃ (65 wt%), HF (≥ 40 wt%) and H₂O (volume ratio of 1:1:1), and then rinsed with deionized water repeatedly. After drying, the cleaned Ti foil was sealed in a 50 mL Teflon-lined stainless autoclave with 30 mL 10 M NaOH aqueous solution. After the hydrothermal treatment at 140 °C for 6 h, the product was immersed in 0.1 M HCl aqueous solution for 12 h. and then washed with deionized water and dried at 80°C. Finally, all samples were heated in air in a muffle furnace for 2 h at different temperatures (450 °C, 550 °C, 650 °C, 750 °C).

The crystal structure of the samples were characterized by X-ray diffraction (XRD, DX 2700B, Dandong) with Cu Kα radiation. The morphologies and composition of TiO₂ nanotubes were observed by field-emission scanning electron microscopy (FESEM, Quanta 450, FEI) with energy dispersive X-ray (EDX) spectroscopy. More structure details were detected by high-resolution transmission electron microscope (HRTEM, JEOL2100F) working at 200 kV.

The photocatalytic activity of samples was evaluated by the degradation of methylene blue (MB) under irradiation of a 250 W Xenon lamp (Solar-350, Beijing Nbet) for 3 h. The concentration of MB was measured with the UV-Vis spectrophotometer (UV-6100A, Shanghai Metash).

3. Results and discussion

In order to determine the mechanism of hydrothermal reaction, XRD analysis of Ti foil after hydrothermal treatment with only water washing was carried out. As shown in Fig. 1, main diffraction peaks at $2\theta = 35.1^\circ, 38.5^\circ, 40.2^\circ$ and 53° are originated from Ti substrate (JCPDS No. 44-1294). After hydrothermal treatment for 6 h, some small peaks appear, which are corresponding to the hydrothermal reaction product of Na₂Ti₃O₇ (JCPDS No. 31-1329). This result reveals the growth mechanism of TiO₂ on Ti foils and the hydrothermal reaction process can be described by the following equation:



According to other reports [27], when the Ti foil was treated with acid washing after hydrothermal reaction, exchange process of Na⁺ with H⁺ occurs and Na₂Ti₃O₇ has been converted to H₂Ti₃O₇. With a subsequent calcination, TiO₂ nanotubes with good crystal structure are obtained.

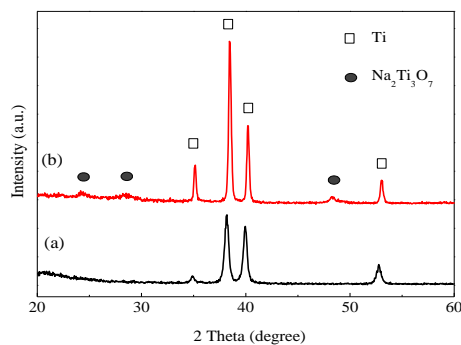


Fig. 1. XRD patterns of (a) Titanium substrate and (b) hydrothermal reaction product.

The XRD patterns of the TiO₂ nanotubes calcined at different temperatures are illustrated in Fig. 2. As the calcination temperature increases from 450°C to 750°C, the intensity of Ti peaks are decreased, instead of the increase of TiO₂ with anatase phase and rutile phase. After calcination at 450°C, the pattern shows the primary diffraction peak (2θ=25.4°) that can be assigned to the anatase phase structure (JCPDS No. 21-1272). With increasing calcination temperature, those peaks associated with anatase phase become sharper, indicating that the crystallinity of TiO₂ is improved. Furthermore, a diffraction peak at 27.5° of rutile phase (JCPDS No. 21-1276) appears when the temperature reached to 650°C. With further increase in temperature at 750°C, the intensity of rutile phase increases greatly, which indicates that most anatase phase has transformed to rutile phase.

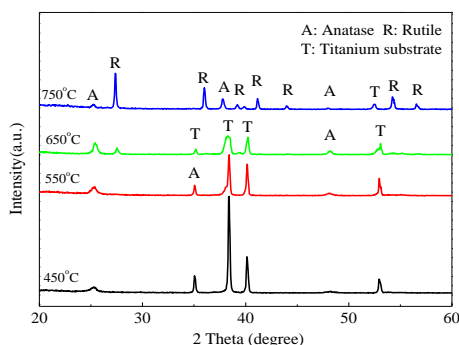


Fig. 2. XRD patterns of TiO₂ nanotubes calcined with different temperatures: (a) 450 °C; (b) 550 °C; (c) 650 °C; (d) 750 °C.

The mean crystallite sizes and relative content of anatase and rutile phase could be calculated by following formulae [28, 29] from the XRD spectra:

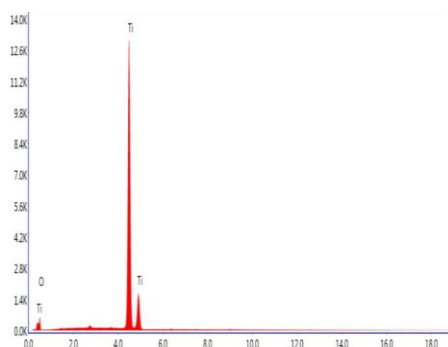
$$D = \frac{0.89\lambda}{B \cos \theta} \quad (1)$$

$$\chi_{rutile} = \frac{1}{1 + 0.8 \frac{I_A}{I_R}} \quad (2)$$

The calculated results are summed in Table 1. It can be seen clearly that both the crystallite size of anatase phase and rutile phase increase with the increasing calcination temperature, which is due to that higher temperature provides more energy to accelerate the growth of crystal grains. Meanwhile as the calcination temperature increases, the content of rutile phase also increases. At a temperature of 750°C, 94.6% anatase phase of TiO₂ has been transformed to rutile phase. It is predictable that when the calcination temperature is improved above 750°C, all anatase phase will be transformed to rutile phase completely.

Table 1. Average crystallization size and phase composition of TiO_2 nanotubes.

| Calcination temperature ($^{\circ}\text{C}$) | Average crystallization size (nm) | | Mass fraction (%) | |
|---------------------------------------------------|-----------------------------------|--------------|-------------------|--------|
| | anatase (101) | rutile (110) | anatase | rutile |
| 450 | 15.5 | — | 100 | — |
| 550 | 16.2 | — | 100 | — |
| 650 | 20.2 | 33.8 | 58.2 | 41.8 |
| 750 | 29.7 | 45.9 | 6.4 | 93.6 |

Fig. 3. EDX spectrum of TiO_2 nanotubes calcined at 450°C .

To further investigate the final product of hydrothermal reaction, EDX spectrum of sample calcined at 450°C is carried out. As shown in Fig. 3, there are only Ti and O elements in the spectrum. It is indicated that sodium ions and hydrogen ions have been removed and TiO_2 nanotubes are obtained by hydrothermal method after ion exchange and calcination process.

Fig. 4 shows the SEM images of TiO_2 nanotubes calcined with various temperatures. As a comparison, a sample without heat treatment was prepared. It can be seen that a uniform film is grown on the surface of Ti foil by hydrothermal method. The diameter of nanotubes is about 10 nm with the length of several dozen micrometers. Comparing with TiO_2 without calcination, there is no obvious difference observed when the sample was calcined at 450°C . As the temperature reaches to 550°C , many tiny nanoparticles appear (Fig. 4(d)), indicated that the nanotube structure is partially destroyed during the process of temperature rising. With further increase in temperature to 650°C , the damage of nanotube structure becomes more serious. Plenty of nanoparticles with average diameter of 20 nm are formed as nodes to split the nanotubes into several parts. Hence the tube length is shortened. At a temperature of 750°C , TiO_2 nanotubes are completely transformed to rod-shaped nanoparticles with diameter of 60 nm approximately. The SEM result shows that the calcination temperature has a great effect on the morphology of TiO_2 nanotubes. At a low temperature under 550°C , the nanotube structure of TiO_2 is remained well. With calcination temperature enhanced, the tubular structure is destroyed and the length is getting shorter. Finally, TiO_2 thin film with nanorods or nanoparticles is obtained, which is explained that the higher temperature offers more energy to fuse the nanotubes structure.

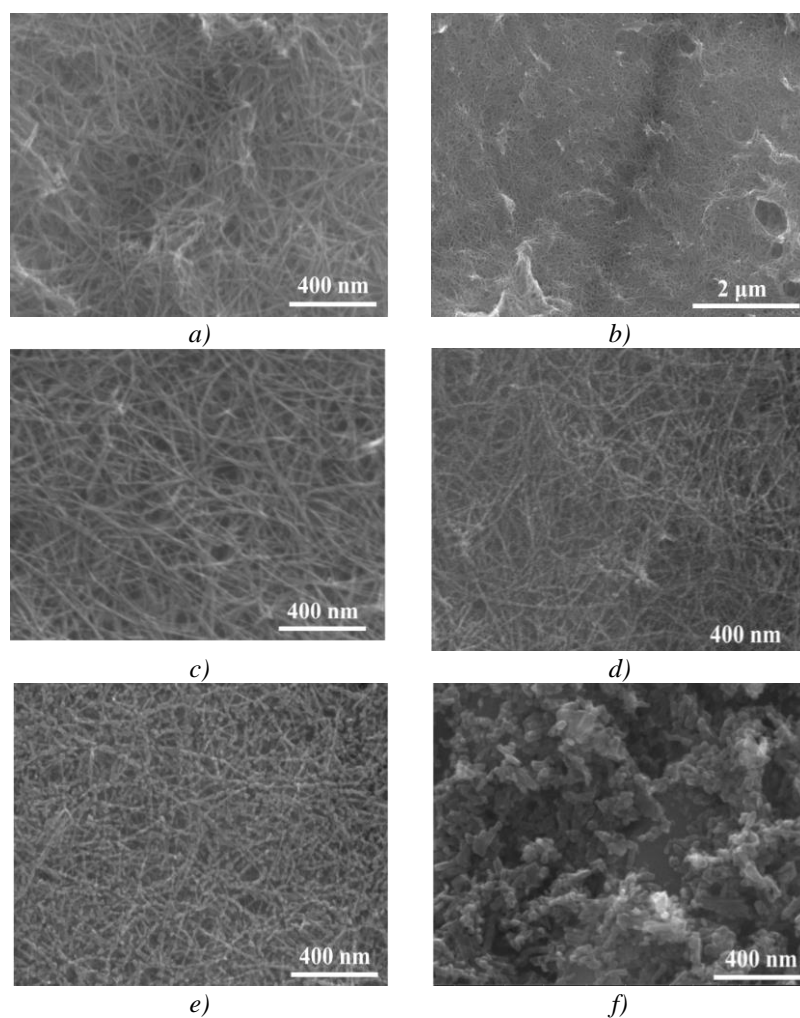


Fig. 4. SEM images of TiO₂ nanotubes prepared with various heat treatment conditions: (a-b) without calcination; (c) 450 °C; (d) 550 °C; (e) 650 °C; (f) 750 °C.

The microstructure of TiO₂ nanotubes annealed at 450 °C is analyzed by TEM and the images are shown in Fig. 5. This result further clarifies that TiO₂ thin film prepared on Ti foil by hydrothermal method in this study is nanotube structure. From the TEM image, a precise diameter of 9 nm of TiO₂ nanotubes is achieved, which is consistent with SEM result.

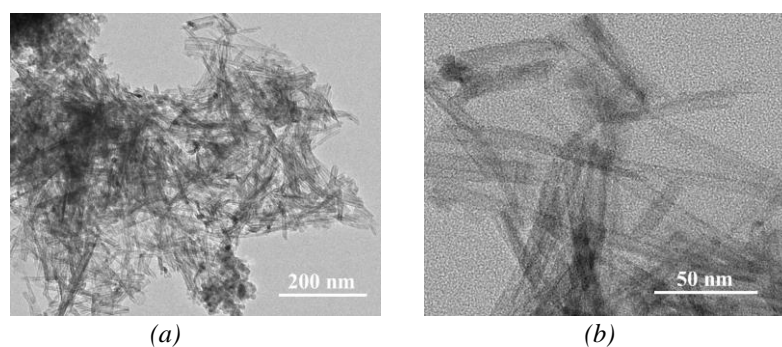


Fig. 5. TEM images of TiO₂ nanotubes annealed at 450 °C.

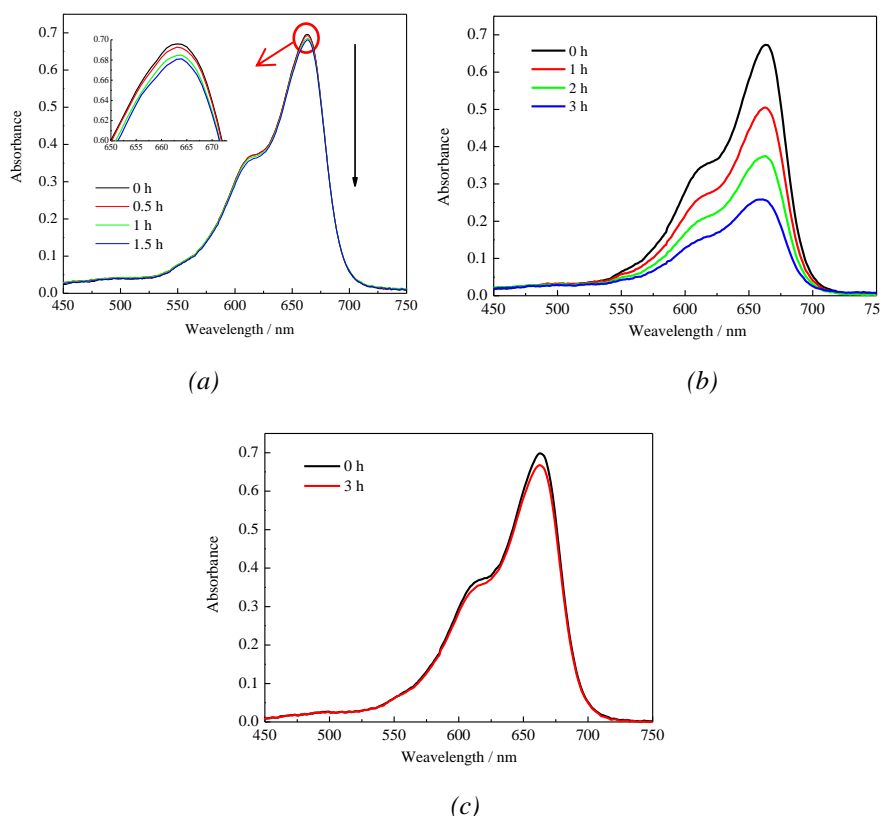


Fig. 6. UV-Vis absorption spectra of MB solution: (a) adsorption behavior of TiO_2 nanotubes calcined at 450°C in the dark; (b) photocatalytic degradation during different irradiation times with TiO_2 calcined at 450°C ; (c) photodegradation of MB without TiO_2 catalyst.

Using MB with a concentration of 10 mg/L as a model pollutant, the photocatalytic activity of TiO_2 nanotubes thin film ($2\text{ cm}\times 1\text{ cm}$) was performed under a 250 W Xenon lamp for 3 hours. Before irradiation, the adsorption equilibrium of MB solution of 50 mL was carried out with TiO_2 nanotubes calcined at various temperatures under dark conditions. The adsorption behavior of TiO_2 nanotubes calcined at 450°C is shown in Fig. 6(a). It is obvious that the absorbance of MB is decreased slightly with adsorption time. After adsorption of 1.5 h, the absorbance of MB only decreases 2.1%, which can be considered as adsorption equilibrium. Fig. 6 (b) shows the absorbance changes of MB solution in the presence of TiO_2 calcined at 450°C with different illumination times. Similar shape curves (not shown here) were obtained by other samples with different calcination temperatures. During the photocatalytic reaction, the absorbance of MB solution constantly decreases with the irradiation time, indicating the decline of MB concentration. The photocatalytic degradation efficiency of TiO_2 nanotubes could be calculated by the following formula:

$$\eta(\%) = \frac{C_0 - C}{C_0} \times 100\% = \frac{A_0 - A}{A_0} \times 100\% \quad (4)$$

where η is the photocatalytic degradation efficiency, C_0 and A_0 are the concentration and absorbance of MB solution after adsorption equilibrium, respectively. C and A are the concentration and absorbance of MB solution after different illumination times.

As a comparison, Fig. 6 (c) shows the photodegradation of MB solution under the same conditions as photocatalytic degradation except the absence of TiO_2 nanotubes. After illumination of 3 h, only 4.1% of MB solution has been degraded. This result indicates that TiO_2 nanotubes

prepared in this study display excellent photocatalytic activity and the degradation of MB dye is the combined action of photocatalyst and self-degradation under illumination conditions.

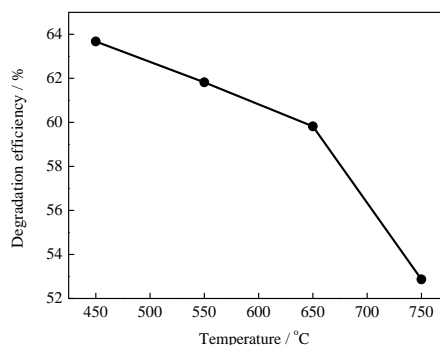


Fig. 7. The photocatalytic degradation activity of TiO₂ nanotubes with different calcination temperatures.

The effect of calcination temperature on the photocatalytic degradation efficiency of TiO₂ nanotubes is investigated in Fig. 7. It can be seen that the degradation efficiency decreases with increasing calcination temperature and TiO₂ nanotubes annealed at 450 °C demonstrates the highest photocatalytic degradation efficiency of 63.7%, which is due to the single crystal structure of anatase phase and the retainment of nanotube structure with higher surface area. As the calcination temperature improved, TiO₂ nanotubes structure is destroyed gradually and the tube diameter becomes larger, leading to the reduction of surface area. Meanwhile much transformation of rutile phase from anatase phase occurred, which is not beneficial for the photocatalytic activity of TiO₂. Therefore, an optimum calcination temperature of 450 °C is acquired.

4. Conclusions

TiO₂ nanotubes were prepared on Ti surface by hydrothermal method. Without acid washing, the hydrothermal product of Na₂Ti₃O₇ is observed and the formation mechanism of TiO₂ nanotubes is also determined. The influence of calcination temperature on the crystal structure, morphology and photocatalytic activity of TiO₂ nanotubes is investigated with various heat treatments. The result indicates that anatase phase begins to transform to rutile phase at 650 °C. At a higher temperature, the destruction of nanotube structure appears and the tube length is shortened. As the calcination temperature reaches to 750 °C, rod-shaped nanoparticles are observed. Consequently, TiO₂ nanotubes calcined at 450 °C demonstrate the highest photocatalytic degradation of MB, which is attributed to the excellent crystal structure and the retainment of nanotube structure.

Acknowledgements

This research was funded by the National Natural Science Foundation of China (No. 51702027).

References

- [1] H. G. Yang, C. H. Sun, S. Z. Qiao, J. Zou, G. Liu, S. C. Smith, H. M. Cheng, G. Q. Lu, *Nature* **453**, 638 (2008).
- [2] J. J. Velazquez, R. Fernandez-Gonzalez, L. Díaz, E. Pulido Melian, V. D. Rodríguez, P. Núñez, *Journal of Alloys and Compounds* **721**, 405 (2017).

- [3] Z. N. Song, M. Fathizadeh, Y. Huang, K. H. Chu, Y. M. Yoon, L. Wang, W. L. Xu, M. Yu, *Journal of Membrane Science* **510**, 72 (2016).
- [4] E. Arcadipane, R. Sanz, M. Miritello, G. Impellizzeri, M. G. Grimaldi, V. Privitera, L. Romano, *Materials Science in Semiconductor Processing* **42**, 24 (2016).
- [5] K. N. Abhinav, P. E. JagadeeshBabu, *Surface & Coatings Technology* **320**, 259 (2017).
- [6] X. Ding, X. B. Huang, J. L. Jin, H. Ming, L. M. Wang, J. Ming, *Journal of Power Sources* **379**, 53 (2018).
- [7] H. Huang, J. G. Yu, Y. P. Gan, Y. Xia, C. Liang, J. Zhang, X. Y. Tao, W. K. Zhang, *Materials Research Bulletin* **96**, 425 (2017).
- [8] T. Zhao, W. Luo, Y. H. Deng, Y. F. Luo, P. C. Xu, Y. Liu, L. J. Wang, Y. Ren, W. Jiang, *Nano Energy* **26**, 16 (2016).
- [9] N. Vaenas, M. Bidikoudi, T. Stergiopoulos, V. Likodimos, A. G. Kontos, P. Falaras, *Chemical Engineering Journal*, **224**, 121 (2013).
- [10] G. Balasubramanian, D. D. Dionysiou, M. T. Suidan, I. Baudin, J. M. La[^]in[^]e, *Applied Catalysis B: Environmental* **47**(2), 73 (2004).
- [11] L. C'urkovic', D. Ljubas, S. Šegota, I. Bac'ic', *Alloys and Compounds* **604**, 309 (2014).
- [12] A. Acquesta, A. Carangelo, T. Monetta, *Metals* **8**(7), 489 (2018).
- [13] O. K. Varghese, M. Paulose, C. A. Grimes, *Nature Nanotechnology* **4**(9), 592 (2009).
- [14] C. Y. Mao, F. Zuo, Y. Hou, X. H. Bu, P. Y. Feng, *Angewandte Chemie* **126**(39), 1 (2014).
- [15] J. Y. Kim, D. K. Lee, H. J. Kim, I. Lim, W. I. Leeb, D. J. Jang, *Journal of Metals Chemistry* **A1**(9) 5982, (2013).
- [16] S. Chatterjee, S. Bhattacharyya, D. Khushalani, P. Ayyub, *Crystal Growth & Design* **10**(3), 1215 (2010).
- [17] Y. Wang, Z. Li, Y. Cao, F. Li, W. Zhao, X. Q. Liu, J. B. Yang, *Journal of Alloys and Compounds* **677**, 294 (2016).
- [18] Y. P. Tang, L. Hong, Q. L. Wu, J. Q. Li, G. Y. Hou, H. Z. Cao, L. K. Wu, G. Q. Zheng, *Electrochimica Acta* **195**, 27 (2016).
- [19] M. Xi, Y. L. Zhang, L. Z. Long, X. J. Li, *Journal of Solid State Chemistry* **219**, 118 (2014).
- [20] M. Qamar, C. R. Yoon, H. J. Oh, N. H. Lee, K. Park, D. H. Kim, K. S. Lee, W. J. Lee, S. J. Kim, *Catalysis Today* **131**(1-4), 3 (2008).
- [21] H. Miao, X. Y. Hu, J. Fan, C. B. Li, Q. Sun, Y. Y. Hao, G. W. Zhang, J. T. Bai, X. Hou, *Applied Surface science* **358**, 418 (2015).
- [22] N. Erdogana, A. Ozturka, J. Park, *Ceramics International* **42**(5), 5985 (2016).
- [23] T. Peng, S. Ray, S. S. Veeravalli, J. A. Lalmana, F. A. Khonsari, *Materials Research Bulletin* **105**, 104 (2018).
- [24] W. Wang, Y. J. Zhou, C. H. Lu, Y. Ni, W. F. Rao, *Materials Letters* **160**, 231 (2015).
- [25] H. Yin, G. Q. Ding, B. Gao, F. Q. Huang, X. M. Xie, M. H. Jiang, *Materials Research Bulletin* **47**(11), 3124 (2012).
- [26] S. Aich, M. K. Mishra, C. Sekhar, D. Satapathy, B. Roy, *Materials Letters* **178**, 135 (2016).
- [27] M. S. Chu, Y. L. Tang, N. N. Rong, X. Cui, F. L. Liu, Y. H. Li, C. Zhang, P. Xiao, Y. H. Zhang, *Materials & Design* **97**, 257 (2016).
- [28] V. Uvarov, I. Popov, *Materials Characterization* **58**, 883 (2007).
- [29] C. S. Kim, I. M. Kwon, B. K. Moon, J. H. Jeong, B. C. Choi, J. H. Kim, H. Choi, S. S. Yi, D. H. Yoo, K. S. Hong, J. H. Park, H. S. Lee, *Materials Science & Engineering C-Materials for Biological Applications* **27**(5-8), 1343 (2007).